Arteriosclerosis, Thrombosis, and Vascular Biology

CLINICAL AND POPULATION STUDIES

Low and Oscillatory Wall Shear Stress Is Not Related to Aortic Dilation in Patients With Bicuspid Aortic Valve

A Time-Resolved 3-Dimensional Phase-Contrast Magnetic Resonance Imaging Study

Lydia Dux-Santoy,* Andrea Guala,* Julio Sotelo, Sergio Uribe, Gisela Teixidó-Turà, Aroa Ruiz-Muñoz, Daniel E. Hurtado, Filipa Valente, Laura Galian-Gay, Laura Gutiérrez, Teresa González-Alujas, Kevin M. Johnson, Oliver Wieben, Ignacio Ferreira-Gonzalez, Arturo Evangelista, José F. Rodríguez-Palomares

OBJECTIVE: To assess the relationship between regional wall shear stress (WSS) and oscillatory shear index (OSI) and aortic dilation in patients with bicuspid aortic valve (BAV).

APPROACH AND RESULTS: Forty-six consecutive patients with BAV (63% with right-left-coronary-cusp fusion, aortic diameter ≤ 45 mm and no severe valvular disease) and 44 healthy volunteers were studied by time-resolved 3-dimensional phase-contrast magnetic resonance imaging. WSS and OSI were quantified at different levels of the ascending aorta and the aortic arch, and regional WSS and OSI maps were obtained. Seventy percent of BAV had ascending aorta dilation. Compared with healthy volunteers, patients with BAV had increased WSS and decreased OSI in most of the ascending aorta and the aortic arch. In both BAV and healthy volunteers, regions of high WSS matched regions of low OSI and vice versa. No regions of both low WSS and high OSI were identified in BAV compared with healthy volunteers. Patients with BAV with dilated compared with nondilated aorta presented low and oscillatory WSS in the aortic arch, but not in the ascending aorta where dilation is more prevalent. Furthermore, no regions of concomitant low WSS and high OSI were identified when BAV were compared according to leaflet fusion pattern, despite the well-known differences in regional dilation prevalence.

CONCLUSIONS: Regions with low WSS and high OSI do not match those with the highest prevalence of dilation in patients with BAV, thus providing no evidence to support the low and oscillatory shear stress theory in the pathogenesis of proximal aorta dilation in the presence of BAV.

VISUAL OVERVIEW: An online visual overview is available for this article.

Key Words: aorta ■ bicuspid aortic valve ■ magnetic resonance imaging ■ mechanical stress ■ regional blood flow ■ thoracic aortic aneurysm ■ vascular remodeling

Patients with a bicuspid aortic valve (BAV) frequently present aortic dilation (60%–84% of cases),[1–3] which is associated with life-threatening complications, such as aortic dissection or rupture. Both intrinsic genetically triggered alterations of the aortic wall and altered hemodynamic stressors have been suggested to contribute to aortic dilation in BAV.[4,5] The recent introduction of time-resolved 3-dimensional phase-contrast

Correspondence to Lydia Dux-Santoy, PhD, Department of Cardiology, Hospital Universitari Vall d´Hebron, Paseo Vall d'Hebron 119-129, 08035, Barcelona, Spain, Email lydia.dux@gmail.com; or Andrea Guala, PhD, Department of Cardiology, Hospital Universitari Vall d´Hebron, Paseo Vall d'Hebron 119-129, 08035, Barcelona, Spain, Email andrea.guala@yahoo.com

*L. Dux-Santoy and A. Guala contributed equally to this work and are joint first authors.

The online-only Data Supplement is available with this article at https://www.ahajournals.org/doi/suppl/10.1161/ATVBAHA.119.313636.

For Sources of Funding and Disclosures, see page e19.

© 2019 The Authors. *Arteriosclerosis, Thrombosis, and Vascular Biology* is published on behalf of the American Heart Association, Inc., by Wolters Kluwer Health, Inc. This is an open access article under the terms of the Creative Commons Attribution Non-Commercial License, which permits use, distribution, and reproduction in any medium, provided that the original work is properly cited and is not used for commercial purposes.

Arterioscler Thromb Vasc Biol is available at www.ahajournals.org/journal/atvb

Nonstandard Abbreviations and Acronyms

4D flow MRI	time-resolved 3-dimensional phase-contrast magnetic resonance imaging
AAo	ascending aorta
BAV	bicuspid aortic valve
HV	healthy volunteers
OSI	oscillatory shear index
RL-BAV	BAV with fusion of right and left coronary cusps
RN-BAV	BAV with fusion of right coronary and noncoronary cusps
WSS	wall shear stress

magnetic resonance imaging (4D flow MRI) has permitted substantial advances in the analysis of complex aortic flow characteristics, particularly in patients with BAV. Although no conclusive data on the role of genetics are available,[6] several studies have shown that flow alterations may play a role in the development of aortic aneurysms with different behavior depending on the BAV fusion phenotype.[7–9]

Wall shear stress (WSS) is the most commonly studied flow parameter associated with aortic dilation; however, its specific role in vascular dilation and aneurysm formation remains unclear. In patients with BAV, a high WSS with an asymmetrical distribution has been associated with degradation of the elastic fibers of the aortic wall.[9] From the spatial point of view, both maximum axial and circumferential components of WSS have been associated with aortopathy in patients with BAV.[7,10–12] However, directional variations in WSS throughout the cardiac cycle, as described by the oscillatory shear index (OSI), have also been related to vascular aneurysm formation. Some studies have shown that low WSS and high OSI may activate the atherosclerotic process of the wall, leading to dilation of the arterial vessels,[13] at least in intracranial aneurysm formation.[14] This mechanism has also been suggested to contribute to ascending aorta (AAo) dilation in patients with tricuspid aortic valve.[15,16] However, whether this mechanism may contribute to aortic dilation in patients with BAV remains to be established. Indeed, although WSS has been described in the AAo in several 4D flow MRI studies and related to aortic dilation in patients with BAV,[7,8,10] the role of OSI has been evaluated in very few studies with limited populations.[17,18]

Thus, using 4D flow MRI, this study aimed to analyze regional abnormalities in aortic WSS and OSI to ascertain whether low and oscillatory shear stress is locally associated with aortic dilation in these patients.

MATERIALS AND METHODS

The data that support the findings of this study are available from the corresponding author upon reasonable request.

Highlights

- This study investigates whether regions of concomitant low wall shear stress and high oscillatory shear index are related to aortic dilation in patients with bicuspid aortic valve.
- Patients with bicuspid aortic valve compared with healthy volunteers did not present regions of low and oscillatory shear stress, regardless of the presence of dilation.
- Concomitant low wall shear stress and high oscillatory shear index did not differentiate patients with bicuspid aortic valve either by the presence or absence of ascending aorta dilation or by the different cusp-fusion phenotypes despite the well-known differences in regional dilation prevalence between groups.
- These results do not provide evidence to support a potential role for low and oscillatory shear stress in the development of aortic dilation in patients with bicuspid aortic valve.

Study Population

Patients with BAV with fusion of right and left coronary cusps or right and noncoronary cusps, AAo diameters ≤45 mm and no severe valvular disease (aortic regurgitation ≤III, maximum aortic valve velocity <3 m/s) by echocardiography were consecutively and prospectively recruited between June 2014 and December 2015. Inclusion criteria were age >18 years, no hypertension, no connective tissue disorders, no aortic coarctation or other congenital heart diseases, and no contraindication for cardiac magnetic resonance. Forty-four age-matched healthy volunteers (HV) with a tricuspid aortic valve were studied. The study was approved by the local ethics committee, and informed consent was obtained from all participants.

Cardiac Magnetic Resonance Protocol

Cardiac magnetic resonance studies were performed on a clinical GE 1.5T Signa scanner (General Electric, WI). The protocol included 2-dimensional balanced steady-state free-precession cine images, which were used to assess BAV fusion phenotype and aortic diameters (using the double-oblique cine cardiac magnetic resonance at late diastole) and a time-resolved 3-dimensional phase-contrast MRI acquisition (also known as 4D flow MRI) with retrospective ECG gating during free-breathing. Endovenous contrast was not given.

For 4D flow MRI, data were acquired using the VIPR (vastly undersampled isotropic projection) sequence, a radially undersampled acquisition with 5-point balanced velocity encoding.[19] The acquisition volume included the entire thoracic aorta. Acquisitions were made with an 8-channel cardiac coil using the following parameters: velocity encoding 200 cm/s, field of view 400×400×400 mm, scan matrix 160×160×160 (voxel size 2.5×2.5×2.5 mm), flip angle 8°, repetition time 4.2 to 7.2 ms and echo time 2.2 to 3.6 ms. This data set was reconstructed according to the nominal temporal resolution of each patient and was (5×repetition time) 21 to 36 ms. Reconstructions were performed offline with corrections for background phase, eddy currents and trajectory errors.[19]

Aortic Dilation

To determine the presence of aortic dilation in patients with BAV, maximum diameters at aortic root and mid AAo were adjusted with a logarithm transformation to calculate the *Z* score accounting for sex, age, and body surface area.[20] Aortic dilation was considered when at least one *Z* score was over 2.[3]

WSS and OSI: Computation and Analysis

WSS magnitude and OSI maps were computed from 4D flow acquisitions by applying a 3-dimensional finite-element method, as previously described.[21,22] Briefly, the thoracic aorta was semiautomatically segmented and used to generate a tetrahedral mesh using the iso2mesh Matlab toolbox[23] and Computational Geometry Algorithms Library (http://www.cgal.org). Using cubic interpolation, velocity values were transferred from the 4D flow data to each node of the generated mesh. This flow field was later analyzed in terms of local, spatial, and temporal derivatives to compute WSS magnitude and OSI.

Three anatomic reference points (sinotubular junction, brachiocephalic trunk, and left subclavian artery) were located in the AAo and the aortic arch using 4D flow-derived, phase-contrast enhanced magnetic resonance angiography (Figure 1A). The aortic centerline was automatically computed for each segmented aorta using The Vascular Modeling Toolkit[24] (VMTK, Orobix, Bergamo, Italy; www.vmtk.org) and used to calculate 10 double-oblique analysis planes (orthogonal to the centerline) equally distributed in 2 analysis regions: 6 in the AAo, between the sinotubular junction and the origin of the brachiocephalic trunk, and 4 in the aortic arch between the brachiocephalic trunk and the left subclavian artery (Figure 1B). Each region was further divided into 8 equal segments along the aortic circumference: outer, left-outer, left, left-inner, inner, right-inner (RI), right, right-outer (RO; Figure 1C).

Peak-systolic WSS and OSI values of the contour lumen were interpolated using a cubic spline approximation to 80 points uniformly distributed over each contour. Contour-averaged WSS and OSI were calculated, respectively, as the mean values of WSS and OSI in each contour. Regional values were obtained by averaging over each of the 8 circumferential segments (Figure 1C) and were used to create coregistered WSS and OSI maps, as previously described.[7,12] Maps showing regions of low and oscillatory WSS were obtained as the overlap between regions of low WSS and regions of high OSI.

Statistical Analysis

Continuous variables were expressed as mean±SD. The Shapiro-Wilk test was used to evaluate normal distribution. Differences between groups for continuous parameters were assessed by Student *t* test if they presented a normal distribution and Mann-Whitney *U* test otherwise. χ^2 test was applied for categorical variables, which were reported as percentages. A 2-tailed $P<0.05$ was considered statistically significant. SPSS 19.0 software version (IBM SPSS Statistics, IL) was used for the analysis.

RESULTS

Demographics

Forty-six patients with BAV (63% right and left coronary cusp phenotype, 70% with AAo dilation) and 44 HV completed the study protocol. HV and BAV were matched in terms of age, sex, body surface area, and blood pressure (Table). As expected, BAV had higher diameter and *Z* score at both the aortic root and AAo. Compared with HV, nondilated BAV presented statistically significant differences only in aortic root and AAo diameters ($P=0.039$ and $P=0.002$, respectively) and AAo *Z* score ($P<0.0001$). BAV with fusion of right and left coronary cusps (RL-BAV) and BAV with fusion of right coronary and noncoronary cusps (RN-BAV) patients had similar demographic and clinical conditions, but RN-BAV presented higher systolic blood pressure ($P=0.034$). No differences other than aortic diameters and *Z* scores were obtained when comparing patients with nondilated and dilated BAV.

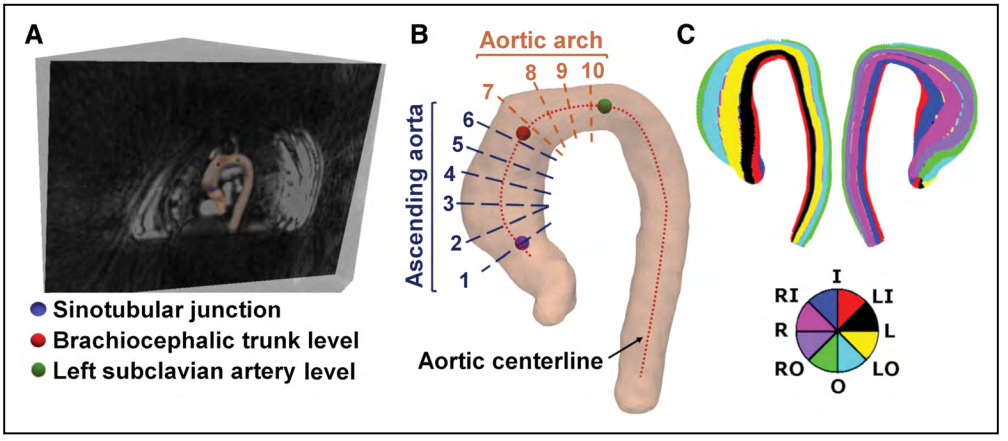

Figure 1. Graphical representation of the analysis regions.
A, Acquired volume containing the segmentation of the aorta and the 3 anatomic reference points: sinotubular junction (blue), the brachiocephalic trunk bifurcation (red), and the left subclavian artery (green). **B**, Using the anatomic references, 6 double-oblique planes (planes 1–6) were distributed in the ascending aorta and 4 (planes 7–10) in the aortic arch. **C**, The aorta was circumferentially divided into 8 segments: outer (O), left-outer (LO), left (L), left-inner (LI), inner (I), right-inner (RI), right (R), right-outer (RO).

Table. Demographics and Aortic Dimensions in HV and Patients With BAV

				BAV Groups					
				BAV Phenotype			BAV Dilation		
	HV	BAV	*P* Value	RL-BAV	RN-BAV	*P* Value	NON-DIL	DIL	*P* Value
N	44	46		29	17		14	32	
Age, y	43±13	45±14	0.404	45±12	46±19	0.795	45±16	46±14	0.865
Men, %	57	59	0.857	62	53	0.544	79	50.0	0.070
BSA, m²	1.8±0.2	1.8±0.2	0.368	1.8±0.2	1.8±0.1	0.678	1.8±0.2	1.8±0.2	0.400
IAo, %			…			0.192			0.103
None	…	30.4		27.6	35.3		28.6	31.3	
Mild	…	50.0		62.1	35.3		42.8	40.6	
Moderate	…	19.6		10.3	29.4		28.6	28.1	
EAo, %			…			0.052			0.332
None	…	93.5		96.6	88.2		100.0	90.6	
Mild	…	6.5		3.4	11.3		0.0	9.4	
SBP, mm Hg	130±19	136±19	0.113	132±17	144±20	0.034	134±17	137±19	0.555
DBP, mm Hg	73±11	76±9	0.125	75±7	79±10	0.105	77±7	76±9	0.861
Diameter SoV, mm	30.5±3.8	35.3±5.1	<0.001	35.4±5.9	35.1±3.4	0.851	33.0±3.6	36.3±5.3	0.040
Diameter AAo, mm	28.2±3.8	38.4±7.2	<0.001	38.0±7.5	39.0±6.7	0.646	32.3±4.1	41.1±6.6	<0.001
Z score SoV	−0.3±1.1	1.21±1.4	<0.001	1.2±1.3	1.2±1.6	0.906	0.3±0.8	1.6±1.4	0.002
Z score AAo	−0.2±0.9	2.7±1.7	<0.001	2.6±1.7	2.9±1.6	0.525	1.0±1.1	3.5±1.3	<0.001

Patients with BAV are compared with HV and according to their fusion phenotype and dilation. Results are presented as mean±SD. *P* value for each comparison are included. AAo indicates ascending aorta; BAV, bicuspid aortic valve; BSA, body surface area; DBP, diastolic blood pressure; DIL, dilated; EAo, aortic stenosis; HV, healthy volunteers; IAo, aortic insufficiency; RL-BAV, BAV with fusion of right and left coronary cusps; RN-BAV, BAV with fusion of right coronary and noncoronary cusps; SBP, systolic blood pressure; and SoV, sinus of Valsalva.

Contour-Averaged WSS and OSI

Contour-averaged WSS magnitude (at peak systole) and OSI were compared between BAV and HV (Figure 2) and in patients with BAV according to the cusp-fusion and the presence of dilation (Figure 3).

Differences Between Patients With BAV and HV

Results of the comparison between BAV and HV, considering the presence of aortic dilation in BAV, are summarized in Figure 2.

Patients with BAV compared with HV presented significantly higher contour-averaged WSS magnitude (Figure 2A, left) but lower OSI (Figure 2A, right) along the whole AAo and the aortic arch. Similar results were obtained when HV with patients with nondilated (Figure 2B) and dilated BAV were compared (Figure 2C). In patients with dilated BAV, however, WSS was slightly decreased in the proximal aortic arch and did not differ from HV in this region (Figure 2C, left).

Differences in Patients With BAV According to Valvular Phenotype and Dilation

When patients with BAV were compared according to the fused cusps, patients with RL-BAV presented higher WSS than RN-BAV in the proximal AAo (Figure 3A, left), with no differences in OSI in this region (Figure 3A, right). Conversely, higher OSI, but similar WSS, was present in the distal AAo and the proximal aortic arch. No statistically significant differences were obtained when patients with BAV were compared according to the presence of aortic dilation (Figure 3B). Nonetheless, both WSS and OSI tended to be lower in the AAo of patients with BAV with a dilated aorta, whereas lower WSS but higher OSI was present in the aortic arch.

Regional WSS and OSI

Figure 4 shows regional WSS and OSI maps in HV and patients with BAV. Moreover, WSS and OSI maps in the subgroups of patients with BAV with and without aortic dilation as well as in patients with BAV according to the leaflet fusion pattern are presented. Corresponding maps of regional statistical differences ($P<0.05$) in WSS and OSI in the comparison between BAV and HV and when patients with BAV were compared according to fused cusps and dilation are shown in Figure 5 and Figure 6, respectively. For all comparisons, the presence of regions with concomitant low WSS and high OSI is also reported in the right panels of Figure 5 and Figure 6.

Differences Between Patients With BAV and HV

In patients with BAV, regional WSS magnitude showed an asymmetrical distribution, with maximum WSS extending from the RI wall in the proximal AAo to the RO wall in the distal AAo (Figure 4B, left). This asymmetry was also present in the aortic arch of BAV but was notably lower

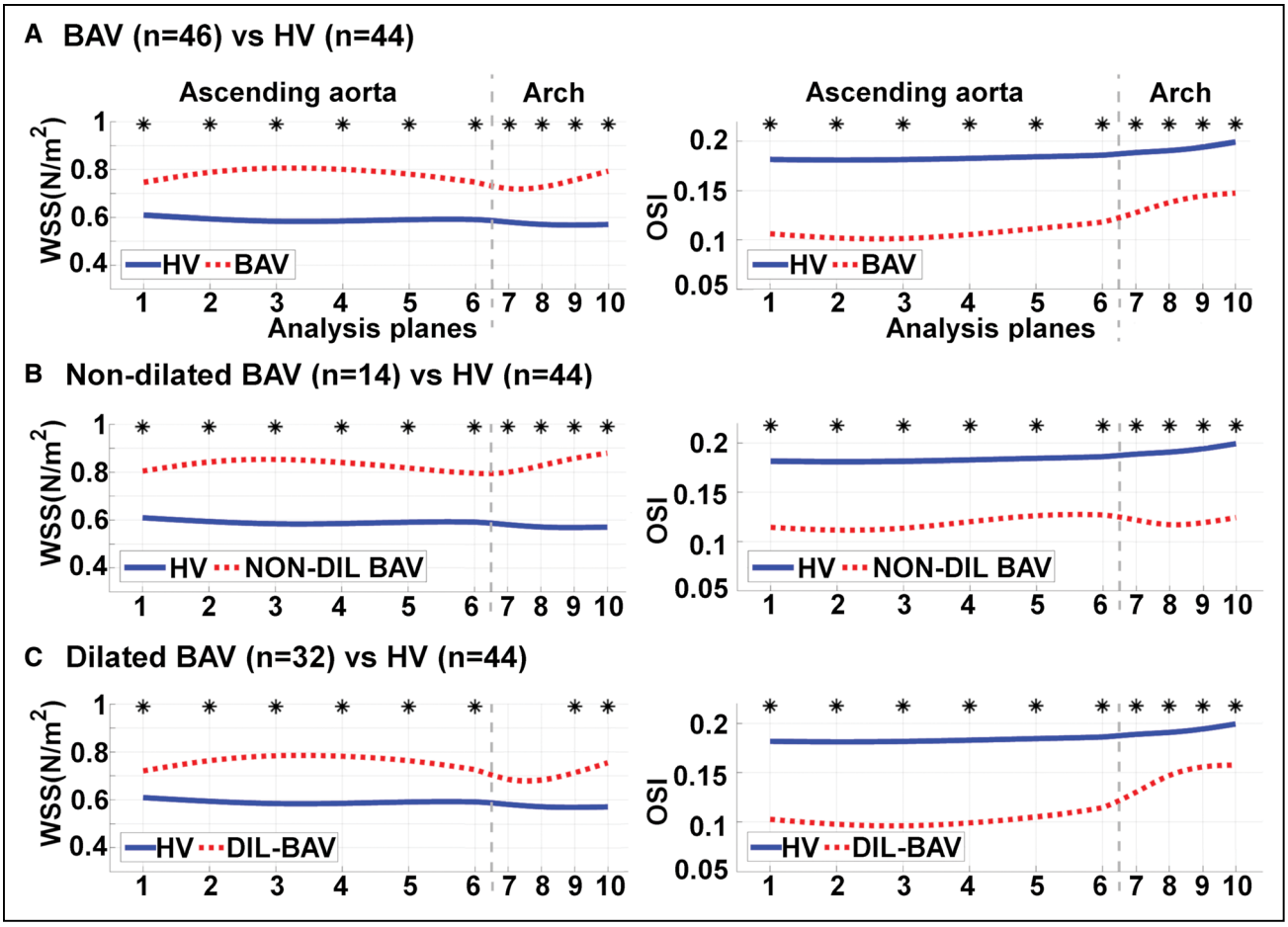

Figure 2. Contour-averaged wall shear stress (WSS) and oscillatory shear index (OSI) comparing patients with bicuspid aortic valve (BAV) and healthy volunteers (HV).
Comparison is performed in the ascending aorta (planes 1-6) and the aortic arch (planes 7-10) of (**A**) patients with BAV vs HV; (**B**) nondilated BAV vs HV; (**C**) dilated BAV vs HV. DIL indicates dilated ascending aorta. *Statistically significant difference ($P<0.05$).

owing to the reduced WSS in this region. By contrast, HV presented homogenously distributed low WSS in the AAo and the aortic arch (Figure 4A, left). Regional OSI maps showed a relative uniform distribution of OSI in HV, which was slightly higher in the left-inner wall along the AAo and the aortic arch (Figure 4A, right). Conversely, BAV showed lower OSI compared with HV, with maximum values extending from the RI mid AAo to RO wall of the aortic arch (Figure 4B, right). Interestingly, regions with lower WSS values matched those with higher OSI and vice versa both in HV (Figure 4A) and BAV (Figure 4B).

Differences in WSS and OSI between HV and BAV emerged in the regional statistical significance maps, where patients with BAV presented higher WSS and lower OSI in most of the AAo and the aortic arch (Figure 5A). Thus, regions of concomitant high WSS and low OSI were obtained in BAV compared with HV (Figure 5A, right). These results were confirmed when patients with nondilated (Figure 4C and Figure 5B) and dilated BAV were compared (Figure 4D and Figure 5C) with HV.

In summary, no regions of concomitant low WSS and high OSI were present in BAV compared with HV, regardless of the presence of dilation.

Differences in Patients With BAV According to Valvular Phenotype and Dilation

Regional WSS and OSI were also analyzed in patients with BAV according to the leaflet fusion pattern (Figure 4E, Figure 4F, and Figure 6B) and the presence or absence of aortic dilation (Figure 4C, Figure 4D, and Figure 6A).

Regional maps presented differences in the extension of high WSS in the different BAV phenotypes, with a maximum WSS extending from the RI wall of the proximal AAo to the RO wall of the mid AAo in RL-BAV (Figure 4E) and from the right wall of the mid AAo to the RO wall in the distal AAo in RN-BAV (Figure 4F). OSI was locally increased only in the distal aortic arch in patients with RN-BAV. Conversely, in patients with RL-BAV, OSI was high along the RI wall of the AAo and the RI to RO wall of the aortic arch (Figure 4F and Figure 4E, respectively). Despite these differences, statistical significance was reached in some regions (Figure 6B, left), but no regions with concomitant low WSS and high OSI were obtained (Figure 6B, right).

Regions of concomitant low WSS and high OSI were only obtained in patients with dilated BAV compared with

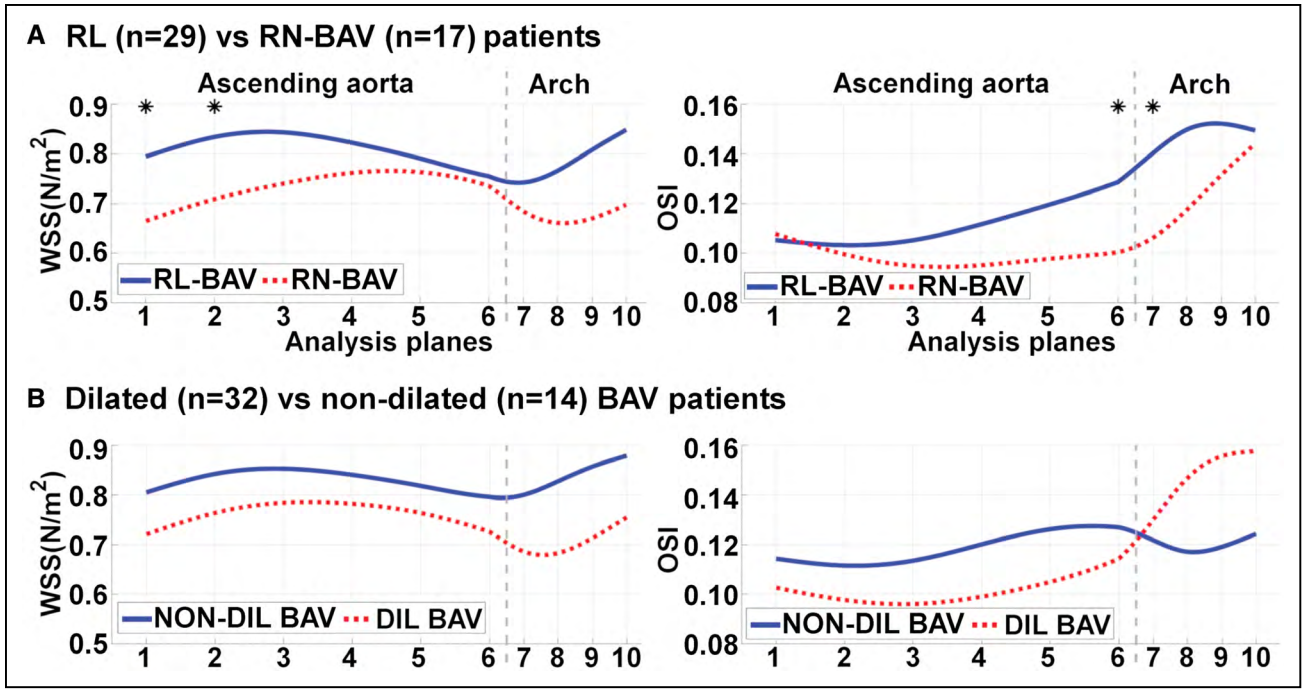

Figure 3. Contour-averaged wall shear stress (WSS) and oscillatory shear index (OSI) in patients with bicuspid aortic valve (BAV) according to their fused cusps and aortic dilation.
Comparison is performed in the ascending aorta (planes 1-6) and the aortic arch (planes 7-10) of (**A**) RL-BAV vs RN-BAV patients and (**B**) BAV patients with nondilated vs dilated aorta. DIL indicates dilated ascending aorta; RL-BAV, BAV with fusion of right and left coronary cusps; RN-BAV, BAV with fusion of right coronary and noncoronary cusps. *Statistically significant difference ($P<0.05$).

nondilated and located in a limited area in the RO wall of the aortic arch (Figure 6A, right).

DISCUSSION

The main findings of our study were (1) patients with BAV did not present regions of concomitant low WSS and high OSI compared with HV, regardless of the presence of dilation; (2) concomitant low WSS and high OSI in the AAo did not differentiate dilated from nondilated patients with BAV or patients with RL-BAV from patients with RN-BAV despite the well-known difference in regional dilation prevalence between these groups; and (3) regions of high OSI matched regions of low WSS magnitude and vice versa. Taken together, these results do not provide evidence to support a potential role for low and oscillatory WSS in the development of BAV aortopathy.

Aortic flow alterations are one of the most important factors related to aneurysm formation in patients with BAV.[7,10,12,25,26] Building from previous studies relating BAV and cusp-fusion phenotypes to regional dilation, this study assessed whether low and oscillatory WSS is related to aortic dilation in BAV. Previous studies related aortic dilation in BAV to high asymmetrical shear stresses resulting from flow eccentricity[7,8] and abnormally increased rotational flow.[7,12] However, other studies showed low and oscillatory WSS to be related to vascular dilation and aneurysm formation through an atherosclerosis-driven process[13,27,28] in the cerebrovascular circulation[14,29] and in the AAo of patients with tricuspid aortic valve.[16] Thus, it is of great interest to assess whether low and oscillatory WSS may also contribute to aortic dilation in BAV. This study evaluates whether this mechanism is related to aortic dilation in patients with BAV.

WSS and OSI in Patients With BAV Compared With HV

In line with previous studies,[8,30] regional WSS magnitude was higher in the RI to RO AAo of patients with BAV compared with HV, regardless of aortic dilation (Figure 5). In HV, the highest OSI was found along the left-inner region of AAo and aortic arch, thus matching with the region where flow tends to separate from the aortic wall.[31] By contrast, in patients with BAV, OSI was higher in the RI to RO wall of the distal AAo and aortic arch (Figure 4B), a result that may be explained by the asymmetrical velocity profile characteristic of patients with BAV. No evidence to sustain the low and oscillatory WSS theory was found in this study. Indeed, no regions with concomitant low WSS and high OSI were observed in patients with BAV compared with HV, while the opposite was true (Figure 5). These results may be partially explained by the strong, inverse relationship between (contour-averaged and regional) WSS and OSI (Figure 4), as previously observed in a small study[17] and confirmed here.

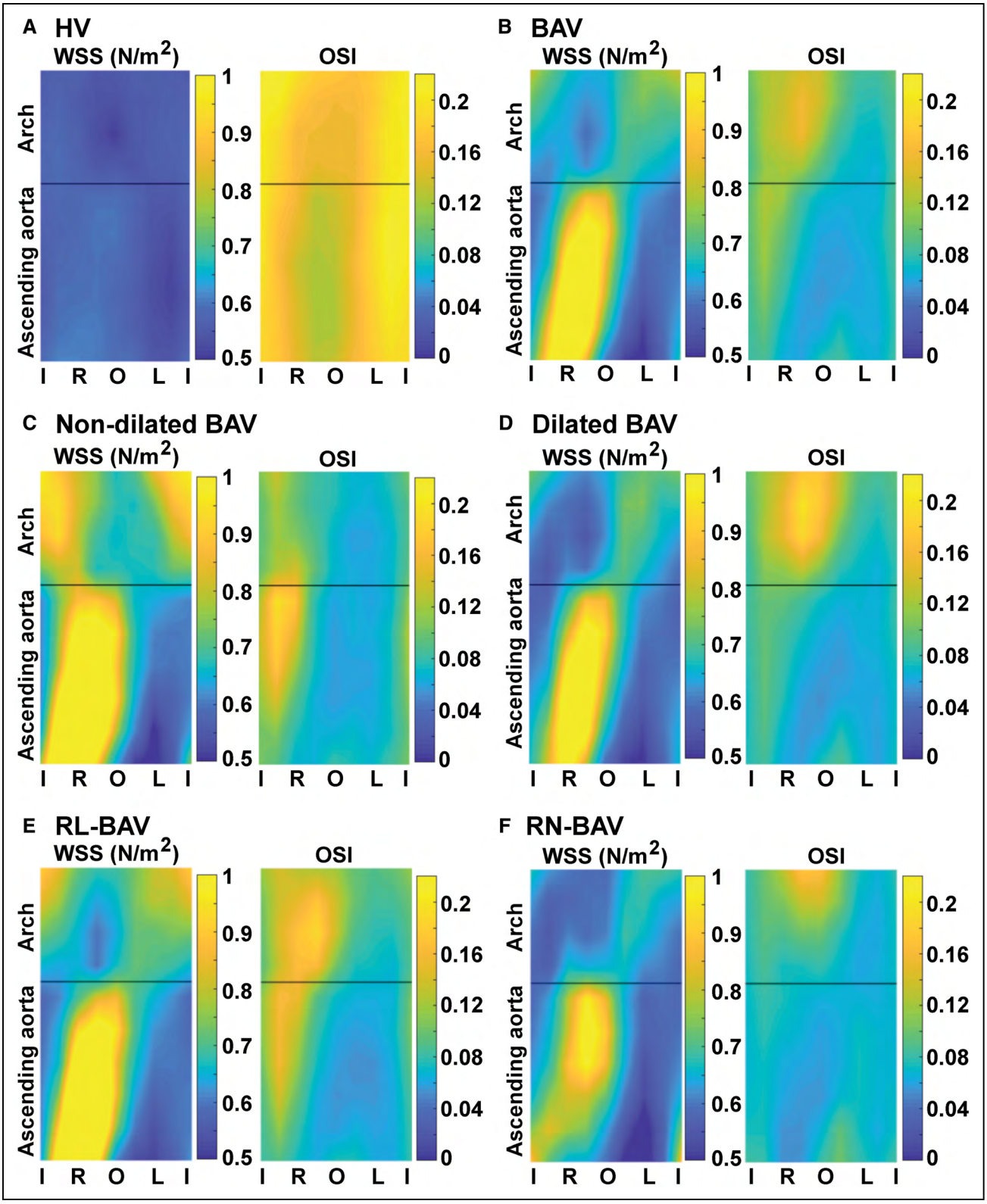

Figure 4. Regional wall shear stress (WSS) and oscillatory shear index (OSI) maps in the ascending aorta and the aortic arch of healthy volunteers (HV) and patients with bicuspid aortic valve (BAV).
HV (**A**); patients with BAV (**B**); BAV with nondilated aorta (**C**); BAV with dilated aorta (**D**); BAV with fusion of right and left coronary cusps (RL-BAV; **E**); BAV with fusion of right coronary and noncoronary cusps (RN-BAV; **F**). I indicates inner; L, left; O, outer; and R, right.

 Arterioscler Thromb Vasc Biol. 2020;40:e10–e20. DOI: 10.1161/ATVBAHA.119.313636

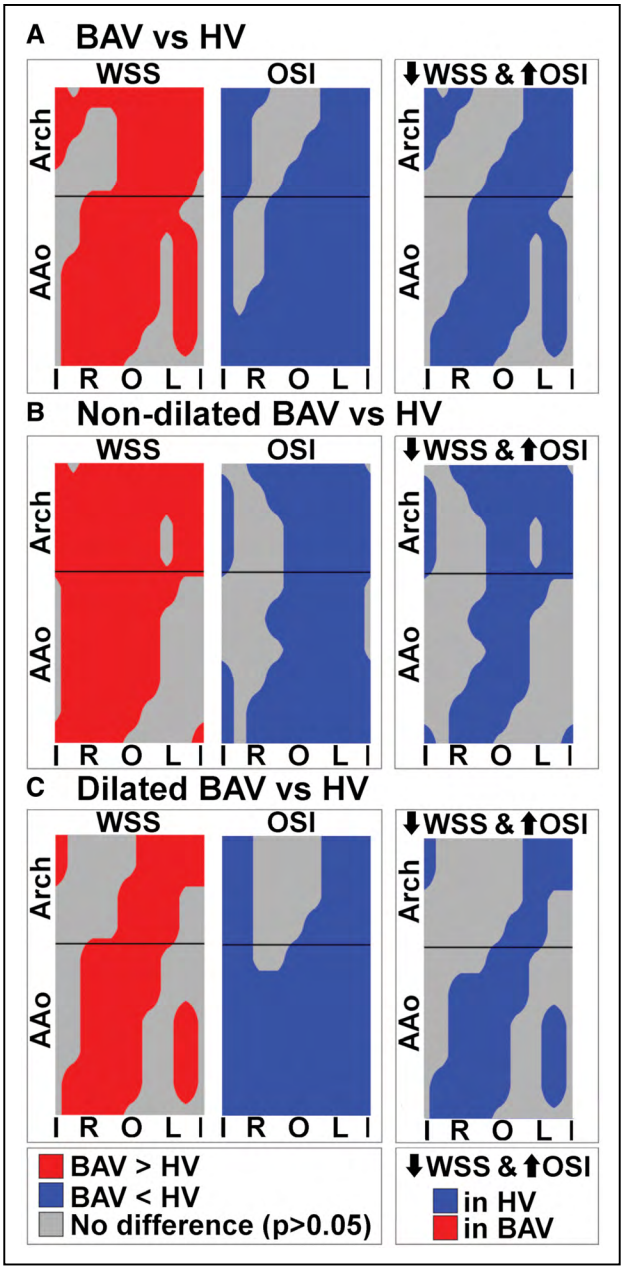

Figure 5. Regional differences in wall shear stress (WSS) and oscillatory shear index (OSI), and regions with concomitant low WSS and high OSI when comparing healthy volunteers (HV) and patients with bicuspid aortic valve (BAV).
BAV vs HV (**A**); BAV with nondilated aorta vs HV (**B**); and BAV with dilated aorta vs HV (**C**). The legend is common for all panels. AAo indicates ascending aorta; I, inner; L, left; O, outer; and R, right.

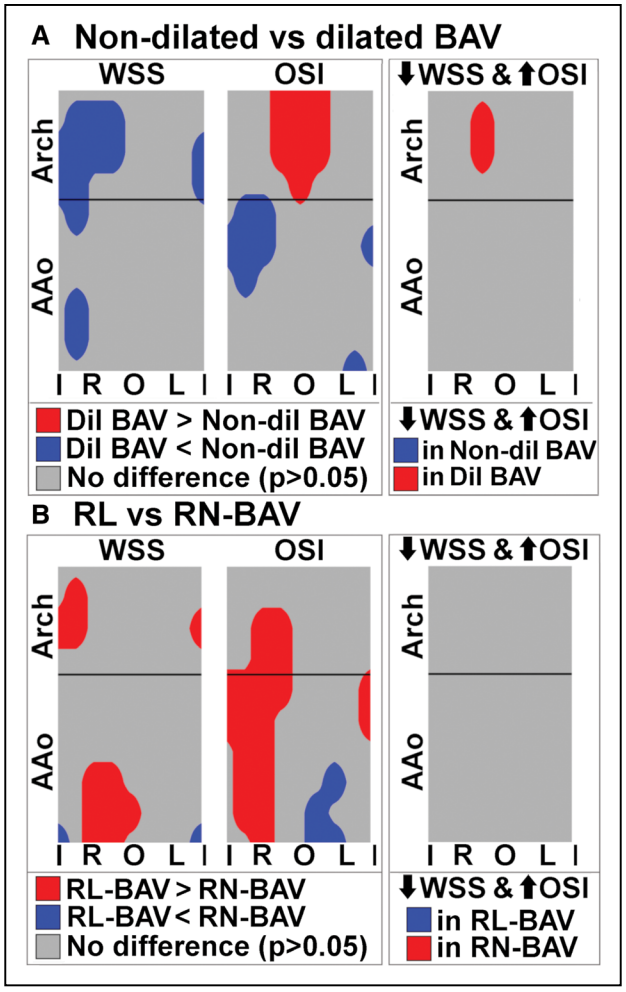

Figure 6. Regional differences in wall shear stress (WSS) and oscillatory shear index (OSI), and regions with concomitant low WSS and high OSI when comparing patients with bicuspid aortic valve (BAV) according to their fused cusps and aortic dilation.
BAV with nondilated vs dilated aorta (**A**), and BAV with fusion of right and left coronary cusps (RL-BAV; **B**) vs BAV with fusion of right coronary and noncoronary cusps (RN-BAV). AAo indicates ascending aorta; I, inner; L, left; O, outer; and R, right.

WSS and OSI in Patients With BAV According to Dilation

Consecutive patients with BAV presented higher OSI in the RI to RO wall of the distal AAo compared with HV. This extends to the very proximal aortic arch in nondilated BAV (Figure 5B, left) and all along the arch in dilated BAV (Figure 5C, left and Figure 6A, left). A small region with both low WSS magnitude and high OSI was thus present in the RO aortic arch of dilated versus nondilated BAV. Bürk et al[16] compared patients with tricuspid aortic valve according to AAo dilation and obtained similar results, thus suggesting a potential role of low WSS and high OSI in aortic dilation. Because increased OSI in the aortic arch is observed in both patients with bicuspid and tricuspid aortic valve only when dilation is present, this characteristic may well be a consequence of dilation. Of note, our data do not concur with a small study in 5 patients with BAV, which reported increased OSI in nondilated BAV.[17] In this context, it is important to underline that flow in the aortic arch is impacted by aortic curvature and the presence of supra-aortic trunks.[28,32] These characteristics may promote local recirculation zones,[33,34] thus creating regions of low and oscillatory WSS[12,32] that may contribute to aortic arch aneurysm formation.[28]

However, considering our results and previous investigations, we conclude that there is not sufficient evidence to support the contribution of this mechanism to aortic dilation in patients with BAV.

WSS and OSI in Patients With BAV According to Cusp-Fusion Phenotype

Maximum regional WSS was obtained in the RI to RO wall of the proximal-mid AAo in RL-BAV and in the RO distal AAo in RN-BAV (Figure 4E and Figure 4F, respectively), matching the outflow jet direction.[7] Regions of relatively high OSI were observed in the mid AAo inner wall of RL-BAV and in the proximal AAo left area of patients with RN-BAV. Of note, these regions showed correspondence with the areas of minimum WSS and did not match areas with different prevalence of dilation between BAV phenotypes (proximal AAo in RL-BAV and distal AAo and proximal aortic arch in RN-BAV[4,12]). Furthermore, no regions of low and oscillatory WSS were identified when BAV phenotypes were compared (Figure 6B, right). These results further downgrade the hypothesis of an etiological role of low and oscillatory WSS for aortic dilation in patients with BAV.

Flow Alterations and Dilation in Patients With BAV

Low and oscillatory WSS has been shown to play a role in atherosclerotic aneurysms[14] and may contribute to thrombus deposition and abdominal aortic dilation.[35] However, our study suggests that this mechanism does not play a role in aortic dilation in BAV. BAV aortic dilation has been previously related to increased flow displacement,[8] increased and asymmetrically distributed WSS,[7,9,36] and increased in-plane and through-plane rotational flow.[7,12] These flow alterations contribute to extracellular matrix dysregulation and elastic fiber degeneration, thereby promoting aortic remodeling.[9] The differences in aortic wall structure at different locations in the aorta and in wall structure, shape, hemodynamic environment, and acting pressure between the aorta and intracranial arteries may well account for a different mechanism in aneurysms etiology.

Limitations

The cross-sectional nature of the present study precludes the investigation of eventual causal relationships. Further longitudinal studies are needed to confirm the results of this study and investigate causal relationships.

Only patients with BAV with nonsevere valvular dysfunction and aortic diameters ≤45 mm were included to limit possible hemodynamic alterations secondary to aortic dilation or severe valvular disease. Moreover, the aortic root was excluded because of poor segmentation quality. Thus, this study cannot rule out a possible role of OSI in patients with BAV with severe valvular disease, larger aortic diameters, or infrequent aortic root dilation.

The number of patients with BAV (46) and HV (44) included in the study is limited, and particularly affects comparisons among BAV subgroups (dilation and valvular phenotype). However, the reliability of the quantitative description of flow characteristics from 4D flow MRI shown in previous studies based on similar or even smaller groups.[8,10,25] should guarantee that the study was powered to detect eventual hemodynamic alterations, as indeed shown for WSS.

Contour-averaging of shear stress measurements leads to the removal of the spatial distribution. To provide regional distribution information of shear stress, all comparisons in the study have been also proposed through regional WSS and OSI maps.

The aortic wall was described using a common segmentation for all cardiac phases. Thus, the calculation of OSI does not account for the aortic movement along the cardiac cycle. Furthermore, results in the aortic arch may be affected by the heterogeneous location of the supra-aortic trunks and aortic curvature. However, as all acquisitions were made using the same imaging parameters and analyzed with the same methods, the comparison between groups was unbiased.

Conclusions

No regions of concomitant low WSS magnitude and high OSI were observed in patients with BAV compared with HV. Although distinct BAV phenotypes are related to different regions of predominant dilation, their comparison in our study did not show regions of concomitant low WSS magnitude and high OSI. These results provide no evidence to support the contribution of low and oscillatory shear stress measures to the pathogenesis of aortic dilation in patients with BAV.

ARTICLE INFORMATION

Received August 8, 2019; accepted November 11, 2019.

Affiliations

From the Department of Cardiology, CIBERCV, Universitat Autònoma de Barcelona, Vall d'Hebron Institut de Recerca (VHIR), Hospital Universitari Vall d´Hebron, Barcelona, Spain (L.D.-S., A.G., G.T.-T., A.R.-M., F.V., L.G.-G., L.G., T.G.-A., A.E., J.F.R.P.); Department of Cardiology, CIBERESP, Universitat Autònoma de Barcelona, Vall d'Hebron Institut de Recerca (VHIR), Hospital Universitari Vall d´Hebron, Barcelona, Spain (I.F.-G.); Biomedical Imaging Center (J.S., S.U.), Department of Electrical Engineering, School of Engineering (J.S.), Department of Radiology, School of Medicine (S.U.), Institute for Biological and Medical Engineering, Schools of Engineering, Medicine, and Biological Sciences (D.E.H.), and Department of Structural and Geotechnical Engineering, Schools of Engineering (D.E.H.), Pontificia Universidad Católica de Chile, Santiago; Millennium Nucleus for Cardiovascular Magnetic Resonance, Santiago, Chile (J.S., S.U., D.E.H.); and Department of Medical Physics (K.M.J., O.W.) and Department of Radiology (K.M.J., O.W.), University of Wisconsin-Madison.

Acknowledgments

We are grateful to Augusto Sao Avilés for statistical analysis and Christine O'Hara for English revisions.

Sources of Funding

This study has been funded by Spanish Ministry of Economy and Competitiveness (RTC-2016-5152-1), Instituto de Salud Carlos III (PI14/0106 and PI17/00381), La Marató de TV3 (project number 20151330) and Centro de Investigación Biomédica en Red - Enfermedades Cardiovasculares (CIBERCV). A. Guala has received funding from the European Union Seventh Framework Programme FP7/People (267128). J. Sotelo, D.E. Hurtado, and S. Uribe were funded by the Millenium Science Initiative of the Ministry of Economy, Development and Tourism, Grant Nucleus for Cardiovascular Magnetic Resonance and projects CONICYT-FONDECYT No. 1181057, Comisión Nacional de Investigación Científica y Tecnológica - Fondo Nacional de Desarrollo Científico y Tecnológico (CONICYT-FONDECYT) Postdoctorado 2017 No. 3170737.

Disclosures

K.M. Johnson has received a research grant from GE Healthcare and from Myocardial Solutions through The University of Wisconsin-Madison (no personal compensation) and holds a consulting agreement with Vertex Pharmaceuticals. O. Wieben has received a research grant from GE Healthcare through The University of Wisconsin-Madison (no personal compensation). The other authors report no conflicts.

REFERENCES

1. Nkomo VT, Enriquez-Sarano M, Ammash NM, Melton LJ 3rd, Bailey KR, Desjardins V, Horn RA, Tajik AJ. Bicuspid aortic valve associated with aortic dilatation: a community-based study. *Arterioscler Thromb Vasc Biol*. 2003;23:351–356. doi: 10.1161/01.atv.0000055441.28842.0a
2. Michelena HI, Khanna AD, Mahoney D, Margaryan E, Topilsky Y, Suri RM, Eidem B, Edwards WD, Sundt TM 3rd, Enriquez-Sarano M. Incidence of aortic complications in patients with bicuspid aortic valves. *JAMA*. 2011;306:1104–1112. doi: 10.1001/jama.2011.1286
3. Evangelista A, Gallego P, Calvo-Iglesias F, Bermejo J, Robledo-Carmona J, Sánchez V, Saura D, Arnold R, Carro A, Maldonado G, et al. Anatomical and clinical predictors of valve dysfunction and aortic dilation in bicuspid aortic valve disease. *Heart*. 2018;104:566–573. doi:10.1136/heartjnl-2017-311560
4. Verma S, Siu SC. Aortic dilatation in patients with bicuspid aortic valve. *N Engl J Med*. 2014;370:1920–1929. doi: 10.1056/NEJMra1207059
5. Guala A, Rodriguez-Palomares J, Dux-Santoy L, Teixido-Tura G, Maldonado G, Galian L, Huguet M, Valente F, Gutiérrez L, González-Alujas T, et al. Influence of aortic dilation on the regional aortic stiffness of bicuspid aortic valve assessed by 4-dimensional flow cardiac magnetic resonance: comparison with marfan syndrome and degenerative aortic aneurysm. *JACC Cardiovasc Imaging*. 2019;12:1020–1029. doi: 10.1016/j.jcmg.2018.03.017
6. Prakash SK, Bossé Y, Muehlschlegel JD, Michelena HI, Limongelli G, Della Corte A, Pluchinotta FR, Russo MG, Evangelista A, Benson DW, et al; BAVCon Investigators. A roadmap to investigate the genetic basis of bicuspid aortic valve and its complications: insights from the international BAVCon (Bicuspid Aortic Valve Consortium). *J Am Coll Cardiol*. 2014;64:832–839. doi: 10.1016/j.jacc.2014.04.073
7. Rodríguez-Palomares JF, Dux-Santoy L, Guala A, Kale R, Maldonado G, Teixidó-Turà G, Galian L, Huguet M, Valente F, Gutiérrez L, et al. Aortic flow patterns and wall shear stress maps by 4D-flow cardiovascular magnetic resonance in the assessment of aortic dilatation in bicuspid aortic valve disease. *J Cardiovasc Magn Reson*. 2018;20:28. doi: 10.1186/s12968-018-0451-1
8. Mahadevia R, Barker AJ, Schnell S, Entezari P, Kansal P, Fedak PW, Malaisrie SC, McCarthy P, Collins J, Carr J, et al. Bicuspid aortic cusp fusion morphology alters aortic three-dimensional outflow patterns, wall shear stress, and expression of aortopathy. *Circulation*. 2014;129:673–682. doi: 10.1161/CIRCULATIONAHA.113.003026
9. Guzzardi DG, Barker AJ, van Ooij P, Malaisrie SC, Puthumana JJ, Belke DD, Mewhort HE, Svystonyuk DA, Kang S, Verma S, et al. Valve-related hemodynamics mediate human bicuspid aortopathy: insights from wall shear stress mapping. *J Am Coll Cardiol*. 2015;66:892–900. doi: 10.1016/j.jacc.2015.06.1310
10. Bissell MM, Hess AT, Biasiolli L, Glaze SJ, Loudon M, Pitcher A, Davis A, Prendergast B, Markl M, Barker AJ, et al. Aortic dilation in bicuspid aortic valve disease: flow pattern is a major contributor and differs with valve fusion type. *Circ Cardiovasc Imaging*. 2013;6:499–507. doi: 10.1161/CIRCIMAGING.113.000528
11. Bieging ET, Frydrychowicz A, Wentland A, Landgraf BR, Johnson KM, Wieben O, François CJ. *In vivo* three-dimensional MR wall shear stress estimation in ascending aortic dilatation. *J Magn Reson Imaging*. 2011;33:589–597. doi: 10.1002/jmri.22485
12. Dux-Santoy L, Guala A, Teixidó-Turà G, Ruiz-Muñoz A, Maldonado G, Villalva N, Galian L, Valente F, Gutiérrez L, González-Alujas T, et al. Increased rotational flow in the proximal aortic arch is associated with its dilation in bicuspid aortic valve disease. *Eur Hear J - Cardiovasc Imaging*. 2019;34:1–11. doi:10.1093/ehjci/jez046
13. Malek AM, Alper SL, Izumo S. Hemodynamic shear stress and its role in atherosclerosis. *JAMA*. 1999;282:2035–2042. doi: 10.1001/jama.282.21.2035
14. Meng H, Tutino VM, Xiang J, Siddiqui A. High WSS or low WSS? Complex interactions of hemodynamics with intracranial aneurysm initiation, growth, and rupture: toward a unifying hypothesis. *AJNR Am J Neuroradiol*. 2014;35:1254–1262. doi: 10.3174/ajnr.A3558
15. Frydrychowicz A, Stalder AF, Russe MF, Bock J, Bauer S, Harloff A, Berger A, Langer M, Hennig J, Markl M. Three-dimensional analysis of segmental wall shear stress in the aorta by flow-sensitive four-dimensional-MRI. *J Magn Reson Imaging*. 2009;30:77–84. doi: 10.1002/jmri.21790
16. Bürk J, Blanke P, Stankovic Z, Barker A, Russe M, Geiger J, Frydrychowicz A, Langer M, Markl M. Evaluation of 3D blood flow patterns and wall shear stress in the normal and dilated thoracic aorta using flow-sensitive 4D CMR. *J Cardiovasc Magn Reson*. 2012;14:84. doi: 10.1186/1532-429X-14-84
17. Piatti F, Sturla F, Bissell MM, Pirola S, Lombardi M, Nesteruk I, Della Corte A, Redaelli ACL, Votta E. 4D flow analysis of BAV-related fluid-dynamic alterations: evidences of wall shear stress alterations in absence of clinically-relevant aortic anatomical remodeling. *Front Physiol*. 2017;8:441. doi: 10.3389/fphys.2017.00441
18. Barker AJ, Lanning C, Shandas R. Quantification of hemodynamic wall shear stress in patients with bicuspid aortic valve using phase-contrast MRI. *Ann Biomed Eng*. 2010;38:788–800. doi: 10.1007/s10439-009-9854-3
19. Johnson KM, Markl M. Improved SNR in phase contrast velocimetry with five-point balanced flow encoding. *Magn Reson Med*. 2010;63:349–355. doi:10.1002/mrm.22202
20. Campens L, Demulier L, De Groote K, Vandekerckhove K, De Wolf D, Roman MJ, Devereux RB, De Paepe A, De Backer J. Reference values for echocardiographic assessment of the diameter of the aortic root and ascending aorta spanning all age categories. *Am J Cardiol*. 2015;114:914–920. doi:10.1016/j.amjcard.2014.06.024
21. Sotelo J, Urbina J, Valverde I, Tejos C, Irarrazaval P, Andia ME, Uribe S, Hurtado DE. 3D quantification of wall shear stress and oscillatory shear index using a finite-element method in 3D CINE PC-MRI data of the thoracic aorta. *IEEE Trans Med Imaging*. 2016;35:1475–1487. doi: 10.1109/TMI.2016.2517406
22. Sotelo J, Dux-Santoy L, Guala A, Rodríguez-Palomares J, Evangelista A, Sing-Long C, Urbina J, Mura J, Hurtado DE, Uribe S. 3D axial and circumferential wall shear stress from 4D flow MRI data using a finite element method and a laplacian approach. *Magn Reson Med*. 2018;79:2816–2823. doi: 10.1002/mrm.26927
23. Qianqian F, Boas DA. Tetrahedral mesh generation from volumetric binary and gray-scale images. *Proc IEEE Int Symp Biomed Imag*. 2009:1142–1145.
24. Antiga L, Piccinelli M, Botti L, Ene-Iordache B, Remuzzi A, Steinman DA. An image-based modeling framework for patient-specific computational hemodynamics. *Med Biol Eng Comput*. 2008;46:1097–1112. doi: 10.1007/s11517-008-0420-1
25. Meierhofer C, Schneider EP, Lyko C, Hutter A, Martinoff S, Markl M, Hager A, Hess J, Stern H, Fratz S. Wall shear stress and flow patterns in the ascending aorta in patients with bicuspid aortic valves differ significantly from tricuspid aortic valves: a prospective study. *Eur Heart J Cardiovasc Imaging*. 2013;14:797–804. doi: 10.1093/ehjci/jes273
26. Guala A, Rodriguez-Palomares J, Galian-Gay L, Teixido-Tura G, Johnson KM, Wieben O, Sao Avilés A, Evangelista A. Partial aortic valve leaflet fusion is related to deleterious alteration of proximal aorta hemodynamics. *Circulation*. 2019;139:2707–2709. doi: 10.1161/CIRCULATIONAHA.119.039693
27. Peiffer V, Sherwin SJ, Weinberg PD. Does low and oscillatory wall shear stress correlate spatially with early atherosclerosis? A systematic review. *Cardiovasc Res*. 2013;99:242–250. doi: 10.1093/cvr/cvt044
28. Cecchi E, Giglioli C, Valente S, Lazzeri C, Gensini GF, Abbate R, Mannini L. Role of hemodynamic shear stress in cardiovascular disease. *Atherosclerosis*. 2011;214:249–256. doi: 10.1016/j.atherosclerosis.2010.09.008
29. Ku DN, Giddens DP, Zarins CK, Glagov S. Pulsatile flow and atherosclerosis in the human carotid bifurcation. Positive correlation between plaque location and low oscillating shear stress. *Arteriosclerosis*. 1985;5:293–302. doi: 10.1161/01.atv.5.3.293
30. van Ooij P, Potters WV, Collins J, Carr M, Carr J, Malaisrie SC, Fedak PW, McCarthy PM, Markl M, Barker AJ. Characterization of abnormal wall shear

stress using 4D flow MRI in human bicuspid aortopathy. *Ann Biomed Eng*. 2015;43:1385–1397. doi: 10.1007/s10439-014-1092-7
31. Vlachopoulos C, O'Rourke MF, Nichols WW. *McDonald's Blood Flow in Arteries: Theoretical, Experimental and Clinical Principles*. 6th ed. London: CRC Press; 2011. doi:10.1201/b13568
32. Kilner PJ, Yang GZ, Mohiaddin RH, Firmin DN, Longmore DB. Helical and retrograde secondary flow patterns in the aortic arch studied by three-directional magnetic resonance velocity mapping. *Circulation*. 1993;88(5 pt 1):2235–2247. doi: 10.1161/01.cir.88.5.2235
33. Richter Y, Edelman ER. Cardiology is flow. *Circulation*. 2006;113:2679–2682. doi: 10.1161/CIRCULATIONAHA.106.632687
34. Guala A, Teixido-Tura G, Dux-Santoy L, Granato C, Ruiz-Muñoz A, Valente F, Galian-Gay L, Gutiérrez L, González-Alujas T, Johnson KM, et al. Decreased rotational flow and circumferential wall shear stress as early markers of descending aorta dilation in Marfan syndrome: a 4D flow CMR study. *J Cardiovasc Magn Reson*. 2019;21:63. doi: 10.1186/s12968-019-0572-1
35. Kontopodis N, Tzirakis K, Ioannou CV. The obsolete maximum diameter criterion, the evident role of biomechanical (Pressure) indices, the new role of hemodynamic (Flow) indices, and the multi-modal approach to the rupture risk assessment of abdominal aortic aneurysms. *Ann Vasc Dis*. 2018;11:78–83. doi: 10.3400/avd.ra.17-00115
36. Barker AJ, Markl M, Bürk J, Lorenz R, Bock J, Bauer S, Schulz-Menger J, von Knobelsdorff-Brenkenhoff F. Bicuspid aortic valve is associated with altered wall shear stress in the ascending aorta. *Circ Cardiovasc Imaging*. 2012;5:457–466. doi: 10.1161/CIRCIMAGING.112.973370